Program Digest, 2019 IEEE International Ultrasonics Symposium (IUS)
Glasgow, Scotland, October 6-9, 2019

Dynamics of Microtubules Disruption and Rearrangement in the Sonoporated Human Umbilical Vein Endothelial Cells

Jianmin Shi[1], Caixia Jia[1], Tao Han[1], Alfred C H Yu[2], Peng Qin[1*]

1. Department of Instrumentation Science and Engineering, Shanghai Jiao Tong University, Shanghai, China

2. Department of Electrical and Computer Engineering, University of Waterloo, Waterloo, ON, Canada

*Corresponding author, E-mail: pqin@sjtu.edu.cn

***Abstract* — The aim of this study was to investigate the response of microtubule cytoskeleton of cells to the perforated membrane by acoustic cavitation. The changes of microtubule at subcellular level were observed in real time using an experimental platform of 1.5 MHz ultrasound exposure (13.33 μs duration and 0.70 MPa peak negative pressure). HUVEC cells exhibited different degrees of cell membrane perforation under acoustic cavitation. Our results show that: 1) After acoustic perforation, tubulin simultaneously depolymerizes with cell membrane rupture. 2) In the case of small membrane damage, tubulin could be rapidly repaired with cell membrane repair. 3) In the case of large membrane damage, tubulin could be repaired far behind the membrane repair. 4) After chelating extracellular calcium ions, the cell membrane and tubulin could not be repaired. These results provide clues for exploring the mechanism of cell membrane repair by ultrasound cavitation.**

Keywords—Sonoporation; Microbubbles; Microtubule; Cell membrane resealing;

I. INTRODUCTION

The cell membrane could be perforated by stable and transient cavitation of microbubbles under acoustic stimulation. Previous studies have shown that ultrasound cavitation can The perforated membrane (sonoporation) has shown great therapeutic potential for clinic application, such as enhancing macromolecule delivery into lesions or tissues, opening blood-brain barrier [1,2,3]. However, these application for macromolecular delivery are closely related to the repair of the perforated membrane in a short time.

As we know, cytoskeleton plays a crucial role in membrane repair [4]. Microtubules, as an important component of cytoskeleton, play an important role in maintaining cell morphology, but it is not clear how microtubules play a role in the subsequent biological process after the cell membrane is repaired [5]. Previous studies have shown that EB1 protein guides the aggregation and extension of microtubules in the process of cell membrane repair, but how the extension of microtubules provides cell support and repair in the process of cell membrane re-encapsulation is the focus of the next research [6]. Early experiments used fixed-point laser ablation and capillary needle destruction of cell membranes to observe the repair process of microtubules after injury [6, 7]. However, after the rupture of cell membrane caused by transient cavitation, the repair process may be similar to that of the rupture of cell membrane in human body, and the change of microtubules in this process is closer to the actual situation [8]. Further, calcium ion, as the second messenger of cells, participates in many physiological processes of cells, including cell membrane repair, microtubule aggregation, extension etc [9,10].

The aim of this work is to understand what the behavior of MTs is upon cavitation-perforated membrane, and how the disturbed MTs restores to initial status. Microtubules fluorescent markers were used to observe the dynamics of intracellular microtubules at the single-cell level after ultrasound treatment. Quantitative evaluation of exogenous molecule uptake was used to determine the degree of the perforated membrane.

II. EXPERIMENTAL MATERIALS AND METHODS

A. Cell Culture

Human Umbilical Vein Endothelial Cells， HUVEC (CRL-1730; ATCC) were cultured in ECM (ScienCell） supplemented with 10% FBS (10099; Gibco) and 1% (v/v) penicillin-streptomycin (10378; Gibco) at 37 ° C and 5% CO2. To prepare the experimental samples, the cultured cells were washed with PBS, harvested by trypsin (25200; Gibco), and seeded into a glass bottom cell culture dish with 1 mL of the same culture medium. After one day of culture, a cell monolayer with approximately 70% confluency was obtained on one side of each dish.

B. Microbubbles preparation

Microbubbles were prepared by the thin film hydration method. Specifically, the lipid shell was composed of DSPC, DSPE-PEG2000 and DOTAP at a molar ratio of 90:5:5which were dissolved in chloroform. Using rotary evaporator and vacuum suction for 2 hours, chloroform was removed and lipid films were formed. Add 3ml PBS mixture into the eggplant bottle with prepared membrane, shake it gently, put it into the ultrasonic water bath box, and then conduct ultrasonic treatment for 20 minutes to obtain liposome solution. In the preparation of microbubbles, the liposome solution was added to the glass bottle to oscillate for 20 s at 4500 rpm, so that the lipid shell could encapsulate the gas, thus forming

microbubbles.

C. Ultrasound Exposure and Calibration

A single-pulsed (20-cycle) sinusoidal waveform signal (33120A; Agilent) which was amplified by high voltage broadband amplification (2100L; E&I) was input a single-element transducer (1 MHz center frequency, 6 mm in diameter) (Advanced Devices; Wakefield, MA) to emit ultrasound waves. The peak negative pressure was measured with capsule hydrophone (HGL-0200; ONDA) at different voltage ranges. Based on the measurement results, we selected the position of 8 mm (far-field) away from the transducer as the exposed area. We used a peak negative pressure of 0.7 MPa to induce the inertial collapse of microbubbles.

D. Experimental Platform

As shown in Fig. 1, a customized experimental platform was used for ultrasound exposure and observation of cells. The cultured and labeled cells and microbubbles were placed on a confocal microscope platform (Eclipse-Ti, Nikon, Japan). The transducer is fixed on the manual three-dimensional positioning device at an angle of 45°. The incident surface of the front end of the ultrasonic transducer was immersed in water, and the exposed cell area was 8 mm from the transducer.

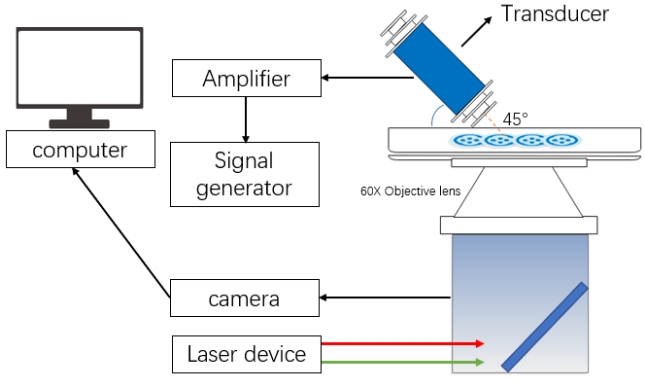

Fig. 1. A customized platform for ultrasound exposure and imaging

E. Sonoporation Probing and Microtubule Observing

80 μM PI (p3566; Invitrogen) was used to track the occurrence of membrane perforation. PI dyes are impermeable into membranes, but they can diffuse into cells under the perforated membranes, and then bind nucleic acids in cytoplasm and nucleus, emitting fluorescence at 610 nm under excitation of 561 nm. The degree of membrane perforation can be evaluated by intracellular PI uptake. Cell viability was evaluated by 0.5 μm Calcein blue AM (C1429; Invitrogen) at 15 minutes after ultrasound treatment. CellLight Tubulin-GFP, BacMam 2.0 (C10509; Invitrogen) was a cell-permeable fluorescent probe to detect the microtubule. 1μl CellLight Tubulin-GFP was added to the cells and mixed gently, and then the cells were returned to culture overnight for the experiments. 575 nm and can be excited by a 488-nm laser.

F. Imaging Acquisition and Data Analysis

A 60× water immersion objective lens (Plane APO, Nikon, Japan) with a 0.31 mm maximum working distance and 1.20 numerical aperture was used to observe images. Bright-field images and basal fluorescence were recorded before ultrasound treatment. A time-lapse model was used to automatically record each set of bright-field, PI and Tubulin-GFP images at different time-points after exposure. The images were taken in 10 s intervals for 1800 s after ultrasound treatment.

The fluorescence images of PI and Tubulin-GFP at different time-points over a 1800 s observation period, and of Calcein Blue at 5 minute post-exposure were quantified to obtain the mean fluorescence intensity using software (NIS-element, Nikon, Japan).

III. Results

A. Microtubule dynamics in different degree of membrane perforation

Different microtubule dynamics were observed in different degree of membrane perforation by collapsing bubbles. As shown by Fig.2B (0s), a single microbubble attached a single cell. The green microbubble cytoskeleton uniformly distributed in the cell. PI fluorescence was not observed in the cells before ultrasound treatment. After ultrasound exposure, as shown in the red arrow of Fig.2C (20s), the extracellular PI locally diffused into the cytosol from the site of the initial bubble, indicated that the cell underwent membrane was perforated by ultrasound-induced microbubble collapse.

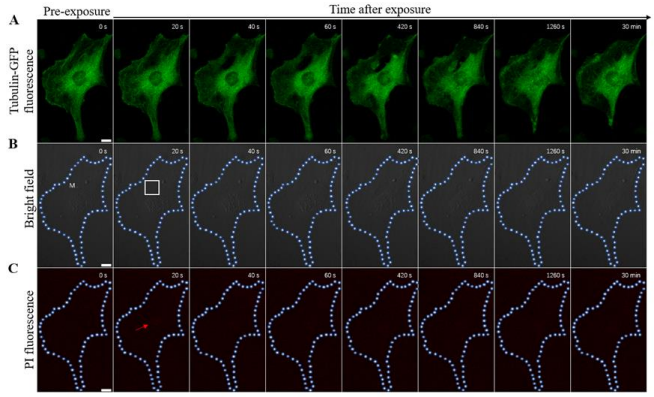

Fig. 2. Time-lapse of long-term microtubule repair of sonoporated cells

Localized microtubule disruption was observed with membrane perforation, As shown by Fig.2A (20s), and then microtubules at the site of perforation gradually depolymerized within the following 40 s, reaching maximum at 60 s post-exposure. In the following about 150 s, PI stopped to permeable into the cells, microtubules began to aggregate, gradually elongate to the perforation site in the next about 30 min. finally, the disrupted microtubule was completely repaired. However, it was noted that PI did not permeate into the cell after about 60s, suggesting that the membrane resealing precedes the microtubule rearrangement.

Another type of microtubule repair, as shown in Fig.3, was achieved the maximum extent of microtubule depolymerization within 40 s after exposure. Self-repair begins after 40 s and

completes the whole repair process in 120 s. Fig.3C (20s) showed that after ultrasound cavitation, minute quantities of PI entered the cell, and then no PI diffused into the cytosol after~100 s. We also found that the microtubule aggregation and extension pattern associated with membrane repair were related to membrane damage. The extent of cell membrane perforation was positively correlated with the repair time of microtubules. In the case of slight perforation, microtubules were repaired rapidly, while in the case of larger perforation, microtubules were repaired slowly.

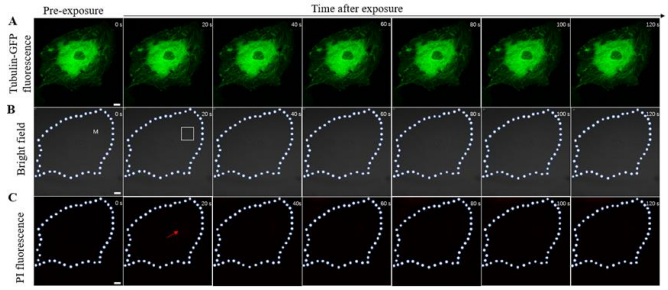

Fig. 3. Time-lapse short term microtubule repair of sonoporated cells

B. *Effect of extracellular calcium chelation on microtubule repairs in Sonoporated Cells*

Next, we determined the dynamics of the microtubules under the absent of the extracellular calcium. The rectangular area in Fig.4B (20s) showed PI rapidly entered into the cytoplasm due to membrane perforation. Simultaneously，similar to the results in the above section, the microtubule structure was locally disrupted with the membrane perforation.

In the following 30 minutes, Intracellular PI continued to increase, suggested that the perforated membrane was not resealed At 35 min post-exposure, almost no Calcein Blue-AM fluorescence was observed in the cell, indicating that the cell lost its viability after extracellular calcium chelated, as shown by Fig.4C (35 min)..Therefore, the cell underwent irreversible membrane perforation. Moreover, during this period, the microtubule structure gradually disintegrated and collapsed, as shown by Fig.4A. Almost no fluorescent signal of tubulin was observed after 30 min post-exposure, suggesting that all microtubules are depolymerized.

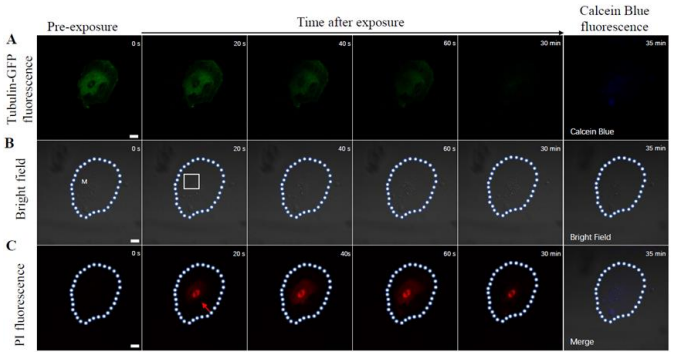

Fig. 4. Time-lapse of calcium chelation treatment microtubule repair of sonoporated cells

IV. Discussion and Conclusion

The dynamics of microtubules in the perforated cells by collapsing bubbles is determined at the single-cell level. Microtubules disrupted rapidly after microbubble collapse, and then the disrupted region gradually extend during the resealing of the perforated membrane, indicative of the depolymerization of microtubules. The extension of the disrupted microtubules is positively correlated with the degree of perforated membrane. The ends of the disrupted microtubules subsequently elongated to repair the disrupted structure. Finally, the disrupted area of microtubules was completely reassembled. We also found the time for microtubules reassembly was far longer than that for the resealing of larger membrane perforation while almost equal to that for the resealing of less membrane perforation.

However, the role of microtubules in the resealing of the perforated membrane, remains unclear. These some key factors related to microtubules rearrangement, such as EB protein family and XMAP protein family which form a complex network with annexin [11], need to be further investigated in future studies.

Acknowledgment

This research is funded by the National Nature Science Foundation of China (No.81471667) and Program of Medicine and Engineering Cross Fund of Shanghai Jiao Tong University (YG2019ZDA27, ZH2018QNA21). SMC Rising Star Fund of Shanghai Jiao Tong University (16X100080028).

References

[1] P. Qin, T. Han, A.Yu, and L.Xu, “Mechanistic understanding the bioeffects of ultrasound-driven microbubbles to enhance macromolecule delivery,” Journal of Controlled Release., vol. 272, no. 2, pp.169–181, Feb. 2018.

[2] P. Qin, L. Xu, Y. Hu, W. Zhong, P. Cai, L. Du, L. Jin, A.C.H. Yu, “Sonoporation-induced depolarization of plasma membrane potential: analysis of heterogeneous impact,” Ultrasound in medicine & biology, vol.40, 2014, pp. 979-989.

[3] P. Qin, L. Xu, T. Han, L.F. Du, A.C.H. Yu, “Effect of non-acoustic parameters on heterogeneous sonoporation mediated by single-pulse ultrasound and microbubbles,” Ultrasonics Sonochemistry, vol.31, 2016, pp.107-115.

[4] Eric Boucher, Craig A. Mandato, “Plasma membrane and cytoskeleton dynamics during single-cell wound healing, ” Biochim Biophys Acta, vol.1853, 2015, pp. 2649-2661.

[5] M.G. Palmisano, S.N. Bremner, T.A. Hornberger, G.A.Meyer, A.A. Domenighetti, S.B. Shah, B. Kiss, M. Kellermayer, A.F. Ryan, R.L. Lieber, “Skeletal muscle intermediate filaments form a stress-transmitting and stress-signaling network, ” Journal of Cell Science, vol. 128, 2015, pp. 219-224.

[6] Tatsuru Togo, “Disruption of the plasma membrane stimulates rearrangement of microtubules and lipid traffic toward the wound site,” Journal of Cell Science, vol. 119, 2006, pp. 2780-2786

[7] Aumeier C, Schaedel L, Gaillard J, John K, Blanchoin L, Théry M, “Self-repair promotes microtubule rescue, ” Nat Cell Biol, vol. 18, 2016, pp. 1054-1064.

[8] P. Campbell, M.R. Prausnitz, “Future directions for therapeutic ultrasound, ” Ultrasound Med Biol, vol.33, 2007, pp. 657.

[9] M.A. Hassan, P. Campbell, T. Kondo, "The role of Ca(2+) in ultrasound-elicited bioeffects: progress, perspectives and prospects, " Drug Discov Today, vol.15, 2010, pp. 892-906.

[10] Alison M.Moe, Adriana E.Golding, William M.Bement, "Cell healing: Calcium, repair and regeneration, " Semin Cell Dev Biol, vol. 45, 2015, pp. 18-23.

[11] Colby P. Fees and Jeffrey K. Moore, "A unified model for microtubule rescue," Molecular Biology of the Cell, vol.30, 2019, pp.753-765.